Coastal Morphodynamic Analysis in Buleleng Regency, Bali - Indonesia

Muh Aris Marfai
Universitas Gadjah Mada Fakultas Geografi
Ratih Winastuti
Universitas Gadjah Mada Fakultas Geografi
Arief Wicaksono
Universitas Gadjah Mada Fakultas Geografi
Bachtiar Wahyu Mutaqin (mutaqin@ugm.ac.id)
Universitas Gadjah Mada https://orcid.org/0000-0002-7667-8411

Research Article

Keywords: morphology, sediment cells, grain size, shoreline change, Buleleng, Indonesia

Posted Date: March 22nd, 2021

DOI: https://doi.org/10.21203/rs.3.rs-277255/v1

Version of Record: A version of this preprint was published at Natural Hazards on November 1st, 2021.
See the published version at https://doi.org/10.1007/s11069-021-05088-8.

Abstract

Sediment as erosion products can affect shoreline, making sediment transport a key process to consider in coastal and shoreline management. Field surveys and secondary data can identify where suspended matters are distributed and deposited to analyze sediment uniformity factors: beach morphology and materials. This research set out to determine the Buleleng Regency's morphodynamic aspects based on the coastal landscape's physical characteristics and the processes acting upon each sediment cell. Field observations were conducted at five stations, from Tukad Gerokgak to Tukad Saba estuary. Jaelani's spectral transformation has been applied to analyze Total Suspended Solids using Sentinel 2A imagery. The laboratory test results of grain-size samples were processed on GRADISTAT, then the depositional environment and sediment transport direction were determined from average grain size, standard deviation, skewness, and kurtosis. Shoreline change, an indicator of coastal morphodynamics, was mapped from Landsat images in 2000, 2008, and 2019 using the Digital Shoreline Analysis System. Statistical analysis on GRADISTAT provided details on depositional environment and sediment transport and deposition based on grain-size distribution. Results indicate poorly sorted medium grain size: gravel (stone) to coarse sand, making up the sediment population from Tukad Gerokgak to Tukad Saba. Generally, sediment is deposited toward coarse, even very coarse, grain on a strongly sloping beach, and there is a high likeliness of sediment accretion. Identified morphodynamic characteristics suggest that the coastal landscape needs structural mitigation to overcome the accelerating impact of human activities and physical processes.

1. Introduction

Coastal areas form at the interface of three major natural systems on earth: atmosphere, ocean, and land surface, which continually change in response to human and natural forces in the form of both physical and non-physical processes, such as storms, currents, erosion, and sedimentation (Weill and Tessier 2016; Mutaqin 2017; Fan et al., 2018; Arjasakusuma et al., 2021). Developing countries, including Indonesia, have reported the most cases of severe natural disaster impacts. Indonesia is particularly vulnerable to sea-level rise, which conduces to erosion and tidal floods (Marfai et al., 2008; Marfai & King 2008a). Flood vulnerability is estimated to worsen in the next 30 years, especially in the coastal urban (Ward et al., 2013).

Changes in a coastal region are closely related to morphology, beach material, and acting process (Bird 2007). A coastal landscape is described through morphodynamic aspects that produce sediment characteristics, beach geometry, and shoreline change. Shoreline change is among the most dynamic processes occurring in it and results from longshore drift, extreme waves, or anthropogenic factors (Bagli & Soille 2003; Mutaqin 2017; Arjasakusuma et al., 2021). Physical processes and human activities have increasingly put pressure on coastal regions and the latter always leave specific features that differ between regions depending on the scale of modification (Lentz & Hapke 2019).

Abrasion and accretion are apparent in the northern coast of Bali Island in Indonesia, notably the Buleleng Regency. Erosion has impacted about 54.83 km or 45% of the regency's shoreline (Heliani et al., 2014). Sea-level rise predictions suggest that about 7.4% of its coast is at risk of inundation, especially Gerokgak and Seririt (Heliani et al., 2014)—two densely populated districts (237 and 652 people/km^2, respectively) with rapid physical development (BPS 2019). In one year (January-December 2019), there were 1,084,168 tourist arrivals, with 29% being international visitors (BPS 2020). Buleleng has grown as a sea transportation node that further generates movements from and to its cargo port in Celukan Bawang, a regional sea port in Sangsit, and a small-sized traditional port in Pengametan Sumberkima.

Coastal area management requires an understanding of the system, including dynamics, interactions, environmental conditions, system sensitivity, and physical processes that shape coastal morphology (Marfai & King 2008b). Although many sediment transport studies have adopted various approaches, the sediment cell has been reported to cover more effective administrative boundaries for shoreline management (Cooper et al., 2002; Collins & Balson 2007). This research has been designed to describe a coastal landscape based on the morphodynamic aspects developing in the Buleleng Regency parts.

2. Methods

The research area is the northern coast of Buleleng Regency, Bali, Indonesia, which administratively covers three districts: Gerokgak, Seririt, and Banjar (Fig. 1). Gerokgak has the longest beach on the island, 76.89 km (BPS 2019). Per the 2018 data of the BPS-Statistics Indonesia, the coastline observed is 157.05 km in length and shows signs of abrasion at varying degrees.

2.1 Data and Tools

The research collected primary data and records from several relevant agencies. Shoreline data were digitized from Landsat images captured on July 17, 2000, July 31, 2008, and April 1, 2019, and downloaded from the USGS website, https://earthexplorer.usgs.gov. SPOT-7 Pansharpen was obtained from LAPAN, while the level-2A Sentinel products recorded on July 20, 2018, and March 27, 2017, were downloaded from https://scihub.copernicus.eu. Landsat is one of the most widely used satellite images for coastal dynamics studies (as a data source) because it is freely available and has long historical data series since 1984 (Pardo-Pascual et al., 2018). Similar studies on shorelines are Duru (2017), Fan et al. (2018), Dewi (2019), Viana-Borja & Ortega-Sanchez (2019), Wicaksono et al. (2019), and Wicaksono & Winastuti (2020). Landsat's main limitation is that the maximum spatial resolution it offers is only up to 30 m, restricting the detection of shoreline changes occurring in a smaller coverage (Pardo-Pascual et al., 2018). Tide predictions were acquired from the Indonesia Geospatial Information Agency (BIG), and data on coastal buildings were from the Center for Coastal Research and Development, Ministry of Public Works and Housing. Other supporting data like wave conditions were measured and documented from wave appearances in the field.

The research mapped shoreline changes from 20-year long data (2000, 2009, and 2019) on the Digital Shoreline Analysis System (DSAS) and conducted observations and measurements in the field for morphodynamics study. DSAS facilitates shoreline mapping and calculation of rates of change (Thieler et al., 2009). Many research works have utilized this application for the same purpose, e.g., Duru (2017), Mutaqin (2017), Dewi (2019), Yulianto et al. (2019), and Wicaksono & Winastuti (2020). Satellite images recorded in the eastern monsoon were selected because they have little to no cloud cover. Likewise, the fieldwork was conducted in the same season because the wave conditions are less extreme than those in the western counterparts.

2.2 Data Processing

a. Digital image processing for shoreline detection used multitemporal Landsat images with a 30m resolution and geometric, radiometric, and atmospheric corrections.

The Modified Normalized Difference Water Index (MNDWI) transformation with a threshold of 0 was applied to these images to determine the boundary line of sea and land in sandy beaches and densely built-up areas. The formula of MNDWI is shown in Equation (1).

$$\text{MNDWI}=\frac{(\text{green}-\text{mid-infrared})}{(\text{green}+\text{mid-infrared})} \quad (1)$$

Xu (2006), Rokni et al. (2014), and Wicaksono & Wicaksono (2019) have justified the application of this method for shoreline identification and suggest that MNDWI gives good results when used for distinguishing between sea and land features in both built-up and open land (sand).

b. Shoreline change was calculated using an additional plug-in on ArcGIS, i.e., DSAS. DSAS contains statistical features useful for this purpose, namely Shoreline Change Envelope (SCE), Net Shoreline Movement (NSM), and End Point Rate (EPR). The formula of each statistical feature is presented below.

SCE= the largest difference in the distance across all shorelines (in meters)

NSM= the difference in distance between the oldest and most recent shorelines (in meters)

EPR= the difference in distance between the oldest and most recent shorelines (in meters) divided by the length of time between the two (in years).

c. The Jaelani algorithm is a spectral transformation index developed by Jaelani et al. (2015) to enable Sentinel 2A imagery in building models associated with Total Suspended Solids (TSS), as shown in Equation (2).

$$\log TSS\ (mg/l) = 1.5212 \times (\log Rrs(\lambda 2)/\log Rrs(\lambda 3)) - 0.3698 \quad (2)$$

d. Sediment cells were delineated based on TSS analysis, differences in beach geometry, and the presence of barrier structures.

e. Sediment samples for grain size analysis were tested in the laboratory, and the results were processed on GRADISTAT. Depositional environment and sediment transport direction were determined using several statistical parameters: the average grain size, standard deviation, skewness, and kurtosis. Their mathematical expressions are written in Table 1.

Table 1 Grain Size Parameter Equations

Mean	Sorting	Skewness	Kurtosis
$\bar{x}_a = \frac{\sum fm}{100}$	$\sigma_a = \sqrt{\frac{\sum f(m_m - \bar{x}_a)^2}{100}}$	$Sk_a = \frac{\sum f(m_m - \bar{x}_a)^3}{100{\sigma_a}^3}$	$k_a = \frac{\sum f(m_m - \bar{x}_a)^4}{100{\sigma_a}^4}$

Source: Blott (2001)

Notes:

f: frequency (in percent)

m: midpoint of each class interval (in metrics, mm, or phi units)

2.3 Fieldwork

Field observations were carried out from May 30 until June 2, 2019, at five stations, starting from the first station at the Tukad Gerokgak estuary to the last in the Tukad Saba estuary area (Fig. 2). This period was selected considering the wide shoreline variation over 20 years. This stage observed and validated data processing results from the first stage and collected relevant primary data. The latter was acquired by observing and measuring oceanography aspects: wave conditions and wind direction and speed, and interviewing local people. The research stages are shown in Fig. 3.

3. Results And Discussion

3.1. Sediment Cells

Geological distribution and control play a significant role in shaping coastal morphodynamics (Klein & Menezes 2001; Benedet et al., 2004; Jackson & Cooper 2009; Short 2010; Scott et al., 2011). Understanding the geological conditions of a coastal system is key in predicting the effects of human-environment interaction and temporal changes of the system (Park et al., 2009). Based on the Indonesian geological map, the stratigraphic rock layers found in the Buleleng Regency are composed of breccia, lava, tuff, and lahar scattered almost in the entire regency. Suspected faults in the Gerokgak District area consist of two large faults that lie parallel to the west and east and are parts of the Pulaki Volcano Rock formation, which is made up of breccia and lava. There are two suspected horizontal faults in the western tip of Bali Island (the Prapat Agung Formation is predominantly covered by limestone, and the Palasari Formation consists of sandstone, conglomerate, and reef limestone). Also, there are two other faults

around the Tejakula District, precisely between the Buyan Bratan and Batur Purba Formations (tuff and lahar deposit), and there is a rock stratification structure consisting of tuff and lava from the ancient volcanic rock formation, Buyan Bratan. Most of Buleleng is a hilly area stretching in the south and low-lying land (coast) in the north. Among the hills are several mountains that are no longer active. The type and nature of beach morphodynamics are sensitive to headland spacing, shape, wave obliquity, indentation ratio, nearshore morphology, and substrate control (Klein & Menezes 2001). The coast's shape is categorized as a bay, with tides, waves, and river discharges being the dominant acting processes.

Grain-size distribution is strongly influenced by the type and availability of sediment source material and the processes involved (Folk & Sanders 1978; Mutaqin et al., 2021). Rock formation requires complex geological processes that have lasted for thousands to millions of years. It is estimated that seabed sediment type and distribution from Tukad Gerokgak to Tukad Saba represent geological complexity in parts of Buleleng and its surroundings. Major rivers carry erosion products to the sea, accumulating seabed sediment in Buleleng waters.

A coastal system consists of a number of units related to and associated with many sediment movement processes occurring at different temporal and spatial scales. Sediment cells are seasonal and annual water mass circulations, with wind or currents being the forces responsible for cell formation. They can be interpreted as accumulated nutrients or limited to sediments without nutrient content (Marfai et al., 2018). The sediment cell concept originates in a balance between sediment transport and wave energy-coarse sediment interaction nearshore that transports or deposits sediment at certain limits. Here, cells are associated with sand or gravel movements along the coast or nearshore in one cell that does not significantly affect adjacent cells (Motyka & Brampton 1993).

Sediment motion is not directly apparent on satellite images, but turbidity can be clearly traced. Turbidity level can describe the direction and distribution of suspended solids and identify deposition location, allowing the coast's uniformity limit to be observable (Khakhim et al., 2005). It also enables the zoning of suspended sediment movements. Coastal physical conditions can be recognized from sediment uniformity, particularly its appearance on a satellite image. TSS is sensitive to land input through river flows and displacement caused by sediment resuspension after erosion (Tarigan & Edward 2003). Sediment loads that enter the sea from river estuaries spread depending on river flow discharge, sediment load volume, current, wave, and tide. Upstream river flows carry sediment to the river mouth, and the rest is transported to the sea. There are differences in suspended sediment levels during floods and ebbs. Floods mean that tidal processes dominate the bay, contributing to higher suspended sediment concentration than ebbs (Alongi 1997). During the flood phase, river flows and inland tidal currents meet in the estuary, which accumulates and deposits TSS originating in the land and the sea at this water body.

Five sediment cells were identified from Tukad Gerokgak to Tukad Saba. Their boundaries are a combination of delineated TSS zones (modeling output is shown in Fig. 4a), beach geometry, and barrier

structures. Despite the different physical processes, they are divided into interdependent cells (Dinas Kelautan dan Perikanan 2004). This research determined these boundaries by considering buildings' presence (Fig. 4b) as barriers to sediment transport because of systemic linkages that form new dynamic interaction and interconnection between social characteristics and ecological system (Biggs et al., 2015).

Coastal slope and seabed sediment distribution illustrate shoreline stability. Time scale and land area, the amount of external energy, and beach material resistance determine coastal stability against shoreline change (Diposaptono, 2004). Coastal slopes are linked to sediment type and distribution that cause abrasion and accretion on the beach. The coastal slope (Table 2) in sediment cells 1, 2, and 4 were strongly sloping (14–19%) with a coarse grain texture, and in sample 3, it was moderately sloping (8–12%) with a coarse grain texture. Sediment with coarse fractions is typical of a strongly sloping terrain because as coastal slope increases, more of this sediment will be transported. However, slopes dominated by grains with moderate fractions, such as sediment cell 5, indicate coastal abrasion (sediment transport) that causes sand particles to accumulate near high tide lines and anthropogenic factors that result in the loss of sediment particles with coarse fractions.

Table 2. Coastal slopes and sediment textures

Sediment Cells	Slope Gradient (%)	Coastal Slope Classifications	Texture Classifications
1	16.73%	strongly sloping	Slightly Gravelly Sand
2	14.05%	strongly sloping	Sandy Gravel
3	12.27%	moderately sloping	Gravelly Muddy Sand
4	16.73%	strongly sloping	Sandy Gravel
5	15.83%	strongly sloping	Muddy Sandy Gravel

Source: Primary data processing, 2019

Tukad Gerokgak (sediment cell 1), Tukad Banyuraras (sediment cell 4), and Tukad Saba (sediment cell 5) flow throughout the year with varying discharge. Small discharge in the dry season diminishes river flow's ability to equal the sedimentation rate generated by tides, sea waves, and currents, thus creating a sand-based dam in the river mouth or sand barriers jutting into the sea. The curved coastline in sediment cell 1 has an 11.97 m-wide beach, undulating morphology, and black sand and bomb/lapilli on the surface. Furthermore, flash floods frequently hit Tukad Gerokgak; Fig. 5a and 5b shows mounts of wastes left on the riverbanks—evidence of flash floods that often accumulate litters on their path. In general, the northern coast of Bali has sloping terrain. However, the estuary area tends to be level, which is thought to be the result of sedimentation of mud materials carried by several rivers emptying into the western part of Buleleng, e.g., Gerokgak, Banyuraras, and Saba in the east. Because of intensive sedimentation, the original river's cross-section is not visible. Fig. 5c and 5d shows pictures of the Tukad Gerokgak estuary.

The Tukad Gerokgak estuary has coarse grains and a narrowing river mouth (see Fig. 5c and 5d). Because of its nearly level coastal slope, many people utilize it for residential purposes and as a location to harvest shellfish during low tides and moor their fishing boats. The same condition is also found in the southeastern part of sediment cell 3 (Nusantara Beach). Barriers like sand deposits play an essential role in forming shoreline geometry and are used extensively for human activities (Aagaard et al., 2004).

Barriers can protect physical features of regional development, such as settlements, ports, and other various land use activities. However, in addition to having regulatory ecosystem services, they are among the most dynamic coastal elements and the most vulnerable to sea-level rise. Here, the development is oriented towards settlements and shrimp ponds instead of the tourism industry. Based on oral sources, history saw that development began with shipping activities in North Bali dating back to the 17th century, which is attributed to the Buginese people (Makassar) who migrated to and settled in the Bugis Buleleng Village, Penyabangan, especially in Celukan Bawang Village, and Sumberkima Village (Astiti, 2018).

Sedimentation analysis using the statistical approaches on GRADISTAT provided information on depositional environment and an overview of sediment transport and depositional processes based on grain-size distribution. The frequency distribution of grain size is closely related to the processes, seafloor sediment type, dynamics, and energy in a depositional environment (Carranza-Edwards et al., 2005). Sorting shows the uniformity of grain size in sedimentary rock: the more uniform the grain size, the better the sorting. Sediment sorting in a coastal environment is generally good (Folk 1980), but the sediment analysis results showed that the particles making up the sediment population from Tukad Gerokgak to Tukad Saba had poorly sorted, moderate grain size: mud, fine sand, gravel (rock), and coarse sand. Rocky surfaces were found at almost all observation points, meaning that the sediment population is composed of coarse to moderate fractions, with varying deviations between the mid and mean values of this population—which indicates poorly sorted sediment particles. Sediment distribution also varies: highly concentrated at certain points but evenly distributed as a whole. Sediment is deposited toward coarse, even very coarse, grain.

The statistical calculation results of sample 1 are shown in Table 3. The sample location had a gritty soil texture, i.e., 88% sand was categorized as slightly gravelly sand. This dominant medium-size sand was poorly sorted (328.4 m, with an average diameter of 1.607). The sorting classification showed non-uniformity because of the currents' energy that moved and deposited material on the shoreline. With a skewness of -0.185 m (fine skewed), the flow distribution can separate between fine and coarse particles. Kurtosis showed very leptokurtic sediment.

Table 3 The statistics of seabed sediment samples

Sample	*MEAN*			*SORTING*			*SKEWNESS*			*KURTOSIS*		
	Geo-metric	Loga-rithmic	Class	Geo-metric	Loga-rithmic	Class	Geo-metric	Loga-rithmic	Class	Geo-metric	Loga-rithmic	Class
1	328.4	1.607	Medium Sand	2.660	1.411	Poorly Sorted	-0.185	0.185	Fine Skewed	2.304	2.304	Very Lepto kurtic
2	1,137.8	-0.186	Very Coarse Sand	3.423	1.775	Poorly Sorted	0.090	-0.090	Symmetrical	1.309	1.309	Lepto kurtic
3	111.6	3.164	Very Fine Sand	16.37	4.033	Extremely Poorly Sorted	0.040	-0.040	Symmetrical	0.578	0.578	Very Platy kurtic
4	2,055.1	-1.039	Very Fine Gravel	6.361	2.669	Very Poorly Sorted	0.377	-0.377	Very Coarse Skewed	0.579	0.579	Very Platy kurtic
5	4,530.9	-2.180	Fine Gravel	4.296	2.103	Very Poorly Sorted	-0.317	0.317	Very Fine Skewed	1.076	1.076	Meso kurtic

In general, the sediment in cell 2 was very coarse sand with poor sorting, possibly because currents prevent water flows from properly separating particles. Besides, the sample location was far from sources of alluvial sediment. However, the sediment had symmetrical skewness, just like sample 3. Sample 3 is part of the bay closest to a steam-electric power station in Celukan Bawang. It is called Nusantara Beach, which is currently not managed. However, it is feared that today's coastal condition leans toward unsustainability and contributes to increased vulnerability to the physical aquatic environment in its surroundings, including shoreline shift due to severe abrasion and natural and anthropogenic factors originating in intensive industrial practices and coal shipping that destroys coral reefs. Sediment characteristics that reflect current geological complexity are beginning to change. Coastal problems and management should factor in social aspects. Humans are an essential key in land use development and, thus, a driving factor in socio-ecological systems (Crossland 2005; Mutaqin 2020). Sediment in sample 3 was extremely poorly sorted because it was mixed with coral reefs on the seabed sediments. The bay's deeper areas had finer sediment, whereas the closer areas to the sea (mouth of the bay) had coarser grains. This finding suggests that the sediment comes from the sea and is then transported and finally deposited at the observation points. A high presence of marine biota shells and dead marine organisms categorizes the sediment as biogenic. On the other hand, some sediments nearshore had terrigenous deposits in the form of fine-sized rocks, clay minerals, and plant remains, indicating influence from the land. During low tides, the location of sediment cell 3 turns into a seagrass bed with sea cucumbers in it; its seaward end is up to 1 km from the low tide line in the morning (Fig. 6).

Sediment cell 4 is located in the Tukad Banyuraras estuary. As observed from the remote sensing images, it is very highly dynamic and is separated into two smaller estuaries by a sand bar (Fig. 7). Land utilization, including resort buildings, is believed to induce changes in future beach morphology. Sediment cell 5 is at the Tukad Saba estuary abutted by densely populated slum settlements. Its location had an irregular shoreline and dominant black sand material, with a beach extending up to 19.1 m in width. Waste accumulating in the estuary narrows its size and is thereby considered the factor of the estuary's dynamics; this is in contrast to sample 4, where natural processes are responsible. This narrowing began with piles of garbage washed up by strong winds and flash floods in 2010 and then February 2019. The kurtosis patterns of samples 3 and 4 were classified as very platykurtic, meaning that deeper bathymetry has a more platykurtic grain-size distribution curve and poorer sediment sorting (Folk & Ward 1957; Cadigan 1961). Sample 5 had mesokurtic kurtosis, which shows that coarser sediment (coarse silt) is in line with its texture, i.e., muddy sandy gravel. In sample 5 (very coarse silt), the skewness value approaches the very fine skewed region, while in sample 4 (sandy gravel), it forms a very coarse skewed curve.

3.2. Shorelines

Shoreline change is a natural dynamic phenomenon that is controlled by beach shape, sediment characteristics, climate change, and anthropogenic effects (Duru, 2017). Sediment transport, sea-level changes, and geomorphological characteristics work together to erode the shoreline and shift its position

(Dewi 2019). Based on satellite image analysis, the shoreline observed is 21.02 km in length, stretching from the coordinates 256825.77 to 273052.485 mE and from 9095248.503 to 9095855.771 mN. Each of its segments was affected by abrasion at varying degrees, and only a few show signs of accretion. These indicate intensive abrasion due to cross-shore transport, where most of the lost sand is deposited into the deeper parts of the sea. Therefore, it is implausible that sand returns to its original location due to deep bathymetry at a fairly close horizontal distance. Longshore transport was also found due to severe abrasion in several places after coastal protection structures were added to adjacent regions. Landsat imagery shows shoreline variation in 20 years (2000–2019). Within this period, the shoreline in parts of the Buleleng Regency extended as a result of accretion. After comparing the length of shorelines on multitemporal images, it is apparent that the shoreline grew longer in 20 years, with an increase of 0.875 km. Morphodynamics is not the sole cause of this increase because of the role of anthropodynamic factors, e.g., constructions of ports, docks, and other coastal defense structures. Because the shoreline changes position from time to time, it's monitoring needs to factor in spatial and temporal aspects (Dewi 2019). Moreover, it is a morphological feature that is often used to understand how coastal systems work and how mid- to long-term processes can affect their development (Pardo-Pascual et al., 2018). Fig. 8a shows a significant shift in some parts of the shoreline, and Fig. 8b presents shoreline changes in the entire research area from 2000 until 2019.

Fig. 8b shows the greatest distance between shorelines in 2000, 2008, and 2019. Most of the 119 transects were accreted from 0 to 170.6 m, and a significant change (>8 m) was found almost on the entire shoreline, including bays and headlands. Meanwhile, from 2018 until 2019, the shoreline changed by 0–35.1 m, mostly in the range of 0–4.3 m. Significant changes (>6.4 m) were seen on headlands and estuaries and only in the bay near the steam-electric power station Celukan Bawang.

One transect was set at a length of 350 m and a distance of 200 m to neighboring transects; for the entire length of the shoreline observed, this setting creates 119 transects. On the graph (Fig. 9), positive values indicate accretion, while negative ones show abrasion. Abrasion susceptibility is presented in an EPR graph, with different colors marking different degrees of resultant damages: dark green for mild damage, light green for moderate damage, green-yellow for heavy damage, and orange for very heavy damage, and red for extremely heavy damage.

The largest shoreline change envelopes (SCE) of up to 160 m are on transects 8, 30, 31, 55, 103, and 104 (see Fig. 9) located in bays and river estuaries. Significant shoreline shifts occurred in these locations. As depicted in the NSM graph (shoreline changes in 2000-2019), more shoreline transects extended seaward, with a maximum rate of change (EPR) reaching 9 m/year. As seen on Landsat images, the abrasion susceptibility in 20 years of observation was mainly linked to mild coastal damages due to accretion.

3.3. Bathymetry

Waters around Buleleng had varying depths, from 0 to 236.36 m. The eastern coast was more profound and had a substantially wider depth gradient than the western counterpart (Fig. 10). The latter had a more

gradual and wider change of depth, while the former had a narrower interval of change, except in the southeast, where changes in water depth were regular and gradual and had a wide interval of distance from one water depth to the next.

Morphologically, sample 3 was a very sloping beach with the smallest area. This variation indicates weaker pressure compared to other locations. The results also showed that part of the beach close to the high tide line (0–20 m) had a large slope gradient, while the rest had smaller ones. These slopes are different from the topography of the island as a whole. Shoreline dynamics are mainly influenced by tidal currents, although waves create heavy pressure in certain seasons. Level beach slopes mean that the pressures acting upon them come from currents influenced by tidal waves. Sediment distribution correlates with depth: the more profound the bathymetry, the finer the sediment (Putra & Nugroho 2017).

Correlation of beach slope with sediment type and distribution (see Table 2 and 3) revealed that higher gradient slopes allowed sediment transport with coarse fractions. In general, tide-dominated coasts have a tidal range of above 2 m. The west season, peaking in February, triggers high waves that cause erosion and damage public facilities and residential buildings. Coastal defense structures built to reduce wave energy are engineering conservation made of stones and concrete. This structural mitigation measure is presented in Fig. 11.

The above description indicates that the coastal landscape pattern in the Buleleng Regency is mainly covered by settlements and industrial buildings growing along the shoreline. However, these components cannot develop optimally, unlike in urban areas where the landscape pattern grows following elevations, slopes, and the developments of roads, city centers, airports, and ports (Han et al., 2009). Here, the rapid development of resorts and hotels (see Fig. 7c) leads to extensive land-use conversion, bringing about environmental degradation due to water pollution and seawater intrusion (Gössling 2001; SOPAC-UNEP 2005; Marfai et al., 2020), exacerbated by the impact of groundwater exploitation, land-use change, trade sector, and shipping activities (Marfai 2014). Cultural and natural tourism sectors are the regency's development priority (Astiti 2018). A collaborative approach in enforcing policies that combine institutions and natural sciences can start with studies of changes in coastal areas to realize systematic environmental management (Mazé et al., 2017). Along the shoreline observed, different parties are responsible for shaping the coastal management in their localities: fisher communities in sediment cells 1, 2, and 5, port corporations, and tourism awareness communities (*Pokdarwis*) in sediment cell 3, and local people in sediment cell 4. In the context of coastal management that integrates physical with social processes, institutions play a necessary part in empowering communities, conserving resources, and managing land utilization, including structural mitigation measures constructed according to coastal landscape characteristics and morphodynamics.

4. Conclusion

The coastal landscape, particularly the morphodynamic aspects, of the Buleleng Regency shows that the sediment population from Tukad Gerokgak to Tukad Saba is composed of poorly sorted, medium-size

grains and that, overall, sediment is deposited toward coarse to very coarse grain. Its strongly sloping morphology allows accretion to dominate along the entire shoreline. As identified from Sentinel-2A imagery, for 20 years (2000-2019), shoreline change is mainly caused by accretion (an increase of up to 0.875 km) attributed to morphodynamic and anthropodynamic factors. Landsat image analysis indicates that abrasion is categorically light because accretion dominates the processes acting upon the shoreline. Furthermore, as identified from Sentinel 2A images, the abrasion susceptibility is associated with moderate damage level because massive abrasion occurs in a few locations. The beach material comprises sand and gravel; therefore, large waves can quickly erode the shoreline, warranting the need for structural mitigation.

Declarations

ACKNOWLEDGMENTS

The authors would like to thank the Master Program on Coastal and Watershed Management Planning (MPPDAS), Faculty of Geography, UGM, for providing supporting facilities and assistance during this research. We also thank anonymous reviewers for their helpful comments on this paper.

Author contributions: M.A.M, R.W., and A.W. designed the study with input from B.W.M. All authors carried out the fieldwork and wrote the manuscript together.

Compliance with ethical standards

Conflict of interest: The authors declare that they have no conflict of interest.

Research involving human participants and/or animals: There is no humans or animals were used in this research.

References

Aagaard, T., Jensen, S.G., & Friderichsen, J. 2004. Longshore sediment transport and coastal erosion at Skallingen, Denmark. *Geografisk Tidsskrift-Danish Journal of Geography*, (104), 5–14. https://doi.org/10.1080/00167223.2004.10649499.

Alongi, D.A. 1997. *Coastal Ecosystem Processes*. CRC Press. New York, USA, 448p.

Arjasakusuma, S., Kusuma, S.S., Saringatin, S., Wicaksono, P., Mutaqin, B.W., Rafif, R. 2021. Shoreline Dynamics in East Java Province, Indonesia from 2000 to 2019 Using Multi-sensor Remote Sensing Data. *Land*. 10(2), 100. https://doi.org/10.3390/land10020100.

Astiti, N.K.A. 2018. Optimalisasi Pengelolaan Pelabuhan-Pelabuhan Kuno Di Buleleng Dalam Pengembangan Pariwisata. *Forum Arkeologi*, 31(1): 75. http://doi.org/10.24832/fa.v31i1.516.

Badan Pusat Statistik. 2019. *Kabupaten Buleleng dalam Angka 2018*. Singaraja: BPS Buleleng.

Badan Pusat Statistik. 2020. *Kecamatan Gerokgak Dalam Angka 2019*. Gerokgak: BPS Buleleng.

Bagli, S., & Soille, P. 2003. Morhological automatic extraction of Pan-European coastline from Landsat ETM +images. *International Symposium on GIS and Computer Cartography for Coastal Zone Management*, October 2003, Genova.

Benedet, L., Finkl, C., Klein, A.H.F., 2004. Morphodynamic classification of beaches on the Atlantic coast of Florida: geographical variability of beach types, beach safety and coastal hazards. *Journal of Coastal Research*, SI 39, 360–365. https://www.jstor.org/stable/25741596.

Biggs, R., Schlüter, M., and Schoon, M.L. Ed. 2015. *Principles for building resilience. Sustaining ecosystem services in social-ecological systems*. Cambridge University Press, Cambridge, UK. 311p.

Bird, E. 2007. *Coastal Geomorphology an Introduction*, Second Edition. England: John Wiley and Sons Ltd. 434p.

Blott, S.J. 2001. GRADISTAT: a grain size distribution and statistics package for the analysis of unconsolidated sediments. *Earth Surface Processes and Landforms*, 26(11). 1237-1248. https://doi.org/10.1002/esp.261.

Cadigan, R.A. 1961. Geologic interpretation of grain-size distribution measurements of Colorado plateau sedimentary rocks. *Journal of Geology* 69(2), 121-144. https://www.jstor.org/stable/30057139.

Carranza-Edwards, A., Rosales-Hoz, L., Urrutia-Fucugauchi, J., Sandoval-Fortanel, A., de la Garza, E.M., and Cruz, R.L.S. 2005. Geochemical distribution pattern of sediments in an active continental shelf in Southern Mexico. *Continental Shelf Research* 25(4), 521–537. https://doi.org/10.1016/j.csr.2004.09.013.

Collins, M.B. & Balson, P.S. 2007. Coastal and Shelf Sediment Transport. *Geological Society of London*, (274): 1–5. https://doi.org/10.1144/GSL.SP.2007.274.01.01.

Cooper, N.J., Barber, P.C., Bray, M.J. & Carter, D.J. 2002. Shoreline management plans: A national review and engineering perspective. *Proceedings of the Institution of Civil Engineers - Water and Maritime Engineering*, 154(3): 221–228. https://doi.org/10.1680/wame.2002.154.3.221.

Crossland, I. 2005. Long-term corrosion of iron and copper. *Proceedings - 10th International Conference on Environmental Remediation and Radioactive Waste Management*, ICEM'05, 2005(1): 1402–1408.

Dewi, R.S. 2019. Monitoring long-term shoreline changes along the coast of Semarang. *IOP Conf. Series: Earth and Environmental Science*, 284 012035, pp. 1-9. https://doi.org/10.1088/1755-1315/284/1/012035.

Dinas Kelautan dan Perikanan. 2004. *Pedoman Penyusunan Rencana Pengelolaan Garis Pantai*. Jakarta: Direktorat Pesisir dan Lautan - Ditjen KP3K.

Diposaptono, S. 2004. *Penambangan Pasir dan Ekologi Laut*. Kasubdit Mitigasi Lingkungan Pesisir Pada Direktorat Jenderal Pesisir dan Pulau-Pulau Kecil, Departemen Kelautan Dan Perikanan.

Duru, U. 2017. Shoreline change assessment using multi-temporal satellite images: a case study of Lake Sapanca, NW Turkey. *Environ Monit Assess*, 189(385), pp. 1-14. https://doi.org/10.1007/s10661-017-6112-2.

Fan, Y., Chen, S., Zhao, B., Yu, S., Ji, H. & Jiang, C. 2018. Monitoring tidal flat dynamics affected by human activities along an eroded coast in the Yellow River Delta, China. *Environmental Monitoring and Assessment*, 190(7), 396. https://doi.org/10.1007/s10661-018-6747-7.

Folk, R.L., Ward, W.C. 1957. Brazos River Bar: A Study in the Significance of Grain Size Parameters. *Journal of Sedimentary Petrology*. 27(1): 3–26. https://doi.org/10.1306/74D70646-2B21-11D7-8648000102C1865D.

Folk R.L. & J.E. Sanders. 1978. *Principles of sedimentology*. John Willey and Sons, NY. 792p.

Folk, R.L. 1980. *Petrology of Sedimentary Rocks*. Hemphill Publishing Company, Austin, 184p.

Gössling, S. 2001. The consequences of tourism for sustainable water use on a tropical island: Zanzibar, Tanzania. *Journal of Environmental Management*, 61, 179–191. https://doi.org/10.1006/jema.2000.0403.

Han, J., Hayashi, Y., Cao, X., & Imura, H. 2009. Application of an integrated system dynamics and cellular automata model for urban growth assessment: A case study of Shanghai, China. *Landscape and Urban Planning*, 91(3), 133–141. https://doi.org/10.1016/j.landurbplan.2008.12.002.

Heliani, L.S, Putra, I.W.K.E., & Subaryono. 2014. The Evaluation of the Result of Post-Processing Envisat Satellite Altimetry Data Used for Coastal Area Potential Flood Mapping (Case Study: Coastal Area of Buleleng Regency, Bali, Indonesia). *Procedia Environmental Sciences* 20: 651-657. http://doi.org/10.1016/j.proenv.2014.03.078.

Jackson, D.W.T., Cooper, J.A.G., 2009. Geological control on beach form: accommodation space and contemporary dynamics. *Journal of Coastal Research*, SI 56, 69–72. https://www.jstor.org/stable/25737539.

Jaelani, L.M., Matsushita, B., Yang, W. and Fukushima, T. 2015. An Improved Atmospheric Correction Algorithm for Applying MERIS Data to Very Turbid Inland Waters, *International Journal of Applied Earth Observation and Geoinformation*, 39, 128–141. https://doi.org/10.1016/j.jag.2015.03.004.

Khakhim, N., Dulbahri., Mardiatno, D., & Arminah, V. 2005. Pendekatan Sel Sedimen Menggunakan Citra Penginderaan Jauh sebagai Dasar Penataan Ruang Wilayah Pesisir (Studi Kasus di Pesisir Utara Propinsi Jawa Tengah), *Majalah Geografi Indonesia*, 19(2), 121-140. https://doi.org/10.22146/mgi.13291.

Klein, A.H.F. and Menezes, J.T. 2001. Beach morphodynamics and profile sequence for a head- land bay coast. *Journal of Coastal Research* 17(4), 812–835. https://www.jstor.org/stable/4300242.

Lentz, E.E. and Hapke, C.J. 2019. Geologic framework influences on the geomorphology of an anthropogenically modified barrier island: Assessment of dune/beach changes at Fire Island, New York. *Geomorphology*, 126(1-2), 82–96. http://doi.org/10.1016/j.geomorph.2010.10.032.

Marfai, M.A., King, L., Singh, L.P., Mardiatno, D., Sartohadi, J., Hadmoko, D.S. & Dewi, A. 2008. Natural hazards in Central Java Province, Indonesia: an overview. *Environmental Geology*, 56: 335–351. https://doi.org/10.1007/s00254-007-1169-9.

Marfai, M.A. and King, L. 2008a. Coastal Flood Management in Semarang, Indonesia. *Environmental Geology*, 55, 1507-1518. http://doi.org/10.1007/s00254-007-1101-3.

Marfai, M.A. and King, L. 2008b. Potential vulnerability implications of coastal inundation due to sea level rise for the coastal zone of Semarang city, Indonesia. *Environmental Geology*, 54, 1235–1245. https://doi.org/10.1007/s00254-007-0906-4.

Marfai, M.A. 2014. *Banjir Pesisir: Kajian Dinamika Pesisir Semarang*. Yogyakarta: Gadjah Mada University Press. 153p.

Marfai, M.A., Trihatmoko, E., Sunarto., Wulandari., Risanti, A.A., and Kurniawan, I.A. 2018. Preliminary study of coastal circulation cells in the coastal area of Kendal, Indonesia. *IOP Conf. Series: Earth and Environmental Science*, 148 012016. https://doi.org/10.1088/1755-1315/148/1/012016.

Marfai, M.A., Ahmada, B., Mutaqin, B.W., Windayati, R. 2020. Dive Resort Mapping and Network Analysis: Water Resources Management in Pemuteran Coastal Area, Bali Island, Indonesia. *Geographia Technica*. 15(2), 106-116. http://doi.org/10.21163/GT_2020.152.11.

Mazé, C., Dahou, T., Ragueneau, O., Danto, A., Mariat-Roy, E., Raimonet, M. & Weisbein, J. 2017. Knowledge and power in integrated coastal management. For a political anthropology of the sea combined with the sciences of the marine environment. *Comptes Rendus Geoscience*, 349(6-7), 359–368. https://doi.org/10.1016/j.crte.2017.09.008.

Motyka, J.M. and Brampton, A.H. 1993. *Coastal management: Mapping of littoral cells*. Hydraulics Research, Report SR 328, Wallingford. 102 pp.

Mutaqin, B.W. 2017. Shoreline Changes Analysis in Kuwaru Coastal Area, Yogyakarta, Indonesia: An Application of the Digital Shoreline Analysis System (DSAS). *International Journal of Sustainable*

Development and Planning 12(7), pp. 1203-1214. https://doi.org/10.2495/SDP-V12-N7-1203-1214.

Mutaqin, B.W. 2020. Spatial Analysis and Geomorphic Characteristics of Coral Reefs on the Eastern Part of Lombok, Indonesia. *Geographia Technica*. 15(2), 202-211. http://doi.org/10.21163/GT_2020.152.19.

Mutaqin, B.W., Lavigne, F., Wassmer, P., Trautmann, M., Joyontono, P., Gomez, C., Septiangga, B., Komorowski, J.C., Sartohadi, J., Hadmoko, D.S. 2021. Evidence of unknown paleo-tsunami events along the Alas Strait, West Sumbawa, Indonesia. *Geosciences*. 11(2), 46. https://doi.org/10.3390/geosciences11020046.

Pardo-Pascual, J.E., Sanchez-Garcia, E., Almonacid-Caballer, J., Palomar-Vazquez, J.M., de los Santos, E.P., Fernandez-Sarria, A., and Balaguer-Beser, A. 2018. Assessing the Accuracy of Automatically Extracted Shorelines on Microtidal Beaches from Landsat 7, Landsat 8 and Sentinel-2 Imagery. *Remote Sensing*, 10(2), 326. https://doi.org/10.3390/rs10020326.

Park, J.-Y., Gayes, P.T., Wells, J.T., 2009. Monitoring beach renourishment along the sediment-starved shoreline of Grand Strand, South Carolina. Journal of Coastal Research 25 (2), 336–349. https://www.jstor.org/stable/27698326.

Putra, P.S. & Nugroho, S.H. 2017. Distribusi Sedimen Permukaan Dasar Laut Perairan Sumba, Nusa Tenggara Timur. *Oseanologi dan Limnologi di Indonesia*, 2(3): 49–63. http://doi.org/10.14203/oldi.2017.v2i3.118.

Rokni, K., Ahmad, A., Selamat, A., & Hazini, S. 2014. Water Feature Extraction and Change Detection Using Multitemporal Landsat Imagery. *Remote Sensing*, 6(5), 4173-4189. https://doi.org/10.3390/rs6054173.

Scott, T., Masselink, G., Russel, P., 2011. Morphodynamic characteristics and classification of beaches in England and Wales. *Marine Geology* 286(1-4), 1–20. https://doi.org/10.1016/j.margeo.2011.04.004.

Short, A.D., 2010. Role of geological inheritance in Australian beach morphodynamics. *Coastal Engineering* 57(2), 92-97. https://doi.org/10.1016/j.coastaleng.2009.09.005.

SOPAC–UNEP. 2005. Building Resilience in SIDS: *The Environmental Vulnerability Index: EVI Final Report*. Retrieved from www.sopac.org/evi and www.unep.org.

Tarigan, M.S. & Edward. 2003. Kandungan Total Zat Padat Tersuspensi (Total Suspended Solid) Perairan Raha, Sulawesi Tenggara. *Makara Journal of Science*, 7(3), 109-119. https://doi/org/10.7454/mss.v7i3.362.

Thieler, E.R., Himmelstoss, E.A., Zichichi, J.L., Ergul, A. 2009. *Digital Shoreline Analysis System (DSAS) version 4.0 – An ArcGIS Extension for Calculating Shoreline Change*. Massachusetts: USGS.

Viana-Borja, S.P., & Ortega-Sanchez, M. 2019. Automatic Methodology to Detect the Coastline from Landsat Images with a New Water Index Assessed on Three Different Spanish Mediterranean Deltas,

Remote Sensing, 11(18), 2186. https://doi.org/10.3390/rs11182186.

Ward, P.J., Pauw, W.P., van Buuren, M.W. & Marfai, M.A. 2013. Governance of flood risk management in a time of climate change: the cases of Jakarta and Rotterdam. *Environmental Politics*, 22(3), 518–536. https://doi.org/10.1080/09644016.2012.683155.

Weill, P. & Tessier, B. 2016. Coastal sediment dynamics: Introduction to the thematic issue. *Comptes Rendus Geoscience*, 348(6), 409–410. http://doi.org/10.1016/j.crte.2016.05.001.

Wicaksono, A., & Wicaksono, P. 2019. Akurasi Geometri Garis Pantai Hasil Transformasi Indeks Air pada Berbagai Penutup Lahan di Kabupaten Jepara. *Majalah Geografi Indonesia*, 33(1), 86-94. https://doi.org/10.22146/mgi.36948.

Wicaksono, A., Wicaksono, P., Khakhim, N., Farda, N.M., Marfai, M.A. 2019. Semi-automatic shoreline extraction using water index transformation on Landsat 8 OLI imagery in Jepara Regency, *Proc. SPIE 11372*, Sixth International Symposium on LAPAN-IPB Satellite, 113721I, https://doi.org/10.1117/12.2540967.

Wicaksono, A. & Winastuti, R. 2020. Kajian Morfodinamika Pesisir dan Kerawanan Abrasi di Kabupaten Buleleng, Provinsi Bali, *Prosiding Seminar Nasional Pengelolaan Pesisir dan Daerah Aliran Sungai ke-5*, pp. 132-140.

Xu, H. 2006. Modification of Normalized Difference Water Index (NDWI) to Enhance Open Water Features in Remotely Sensed Imagery. *International Journal of Remote Sensing*, 27(14), 3025-3033. https://doi.org/10.1080/01431160600589179.

Yulianto, F., Suwarsono, Maulana, T., Khomarudin, M.R. 2019. The dynamics of shoreline change analysis based on the integration of remote sensing and geographic information system (GIS) techniques in Pekalongan coastal area, Central Java, Indonesia. *J. Degrade. Min. Land Manage*, 6(3): 1789-1802. https://doi.org/10.15243/jdmlm.2019.063.1789.

Figures

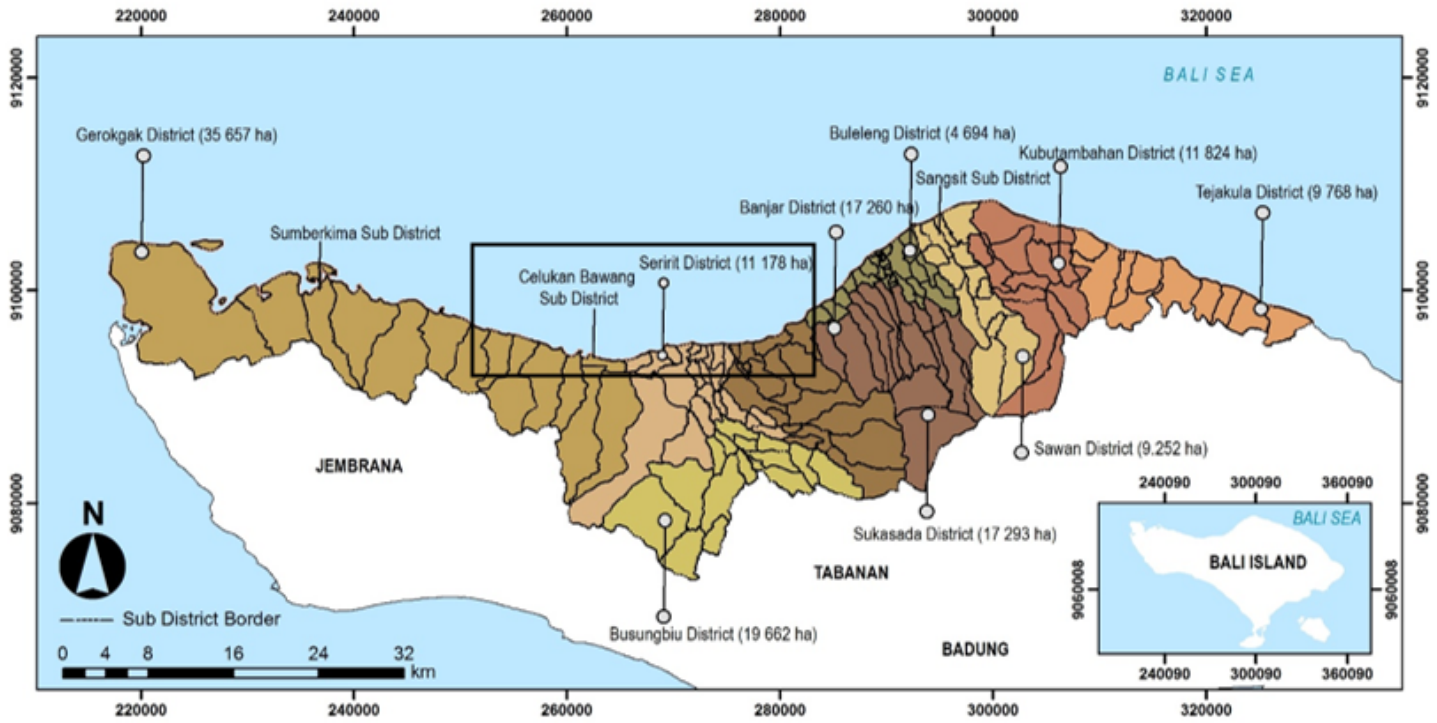

Figure 1

Map of the Buleleng Regency area and the research location. Note: The designations employed and the presentation of the material on this map do not imply the expression of any opinion whatsoever on the part of Research Square concerning the legal status of any country, territory, city or area or of its authorities, or concerning the delimitation of its frontiers or boundaries. This map has been provided by the authors.

Figure 2

Sample distribution during fieldwork

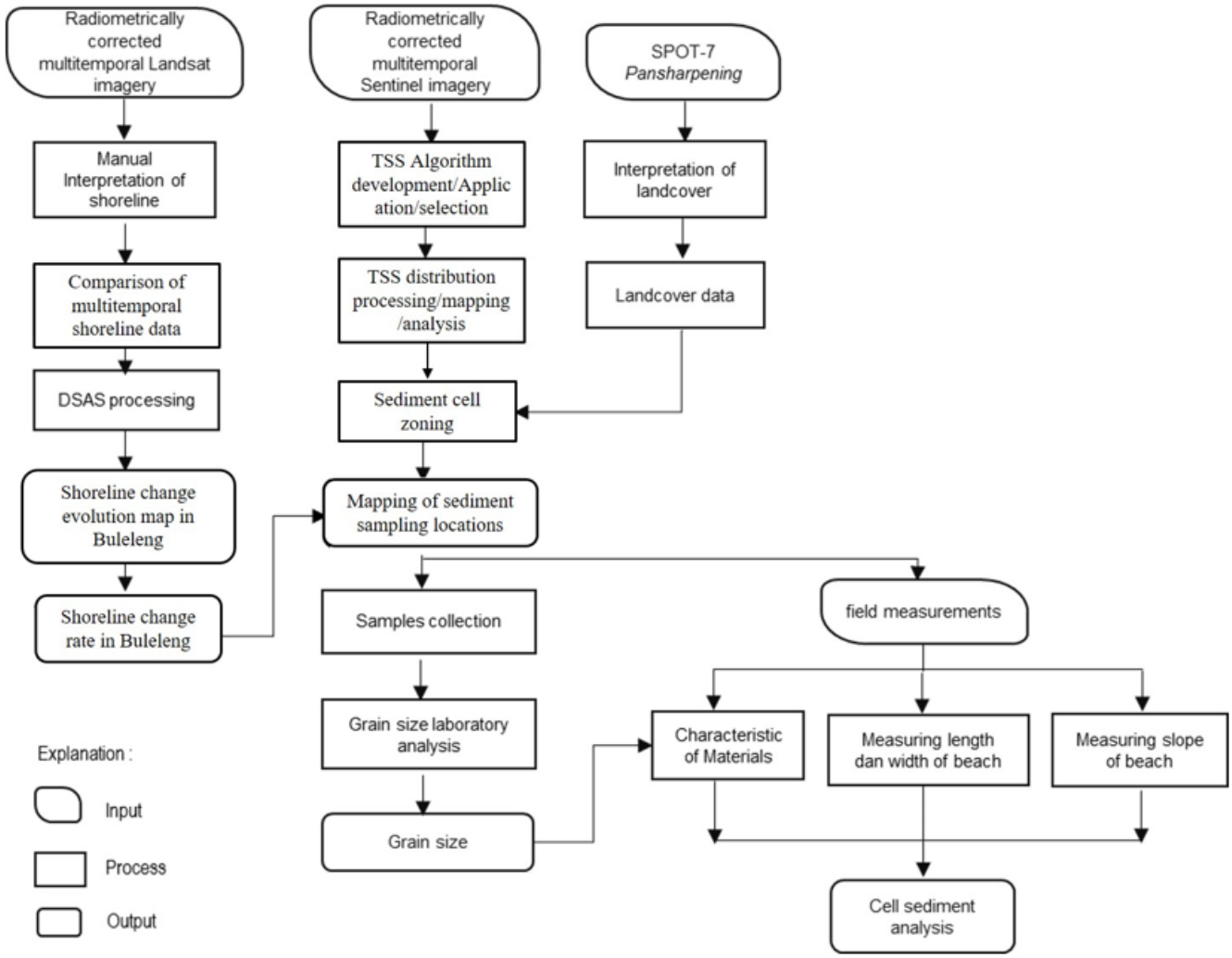

Figure 3

Research flowchart

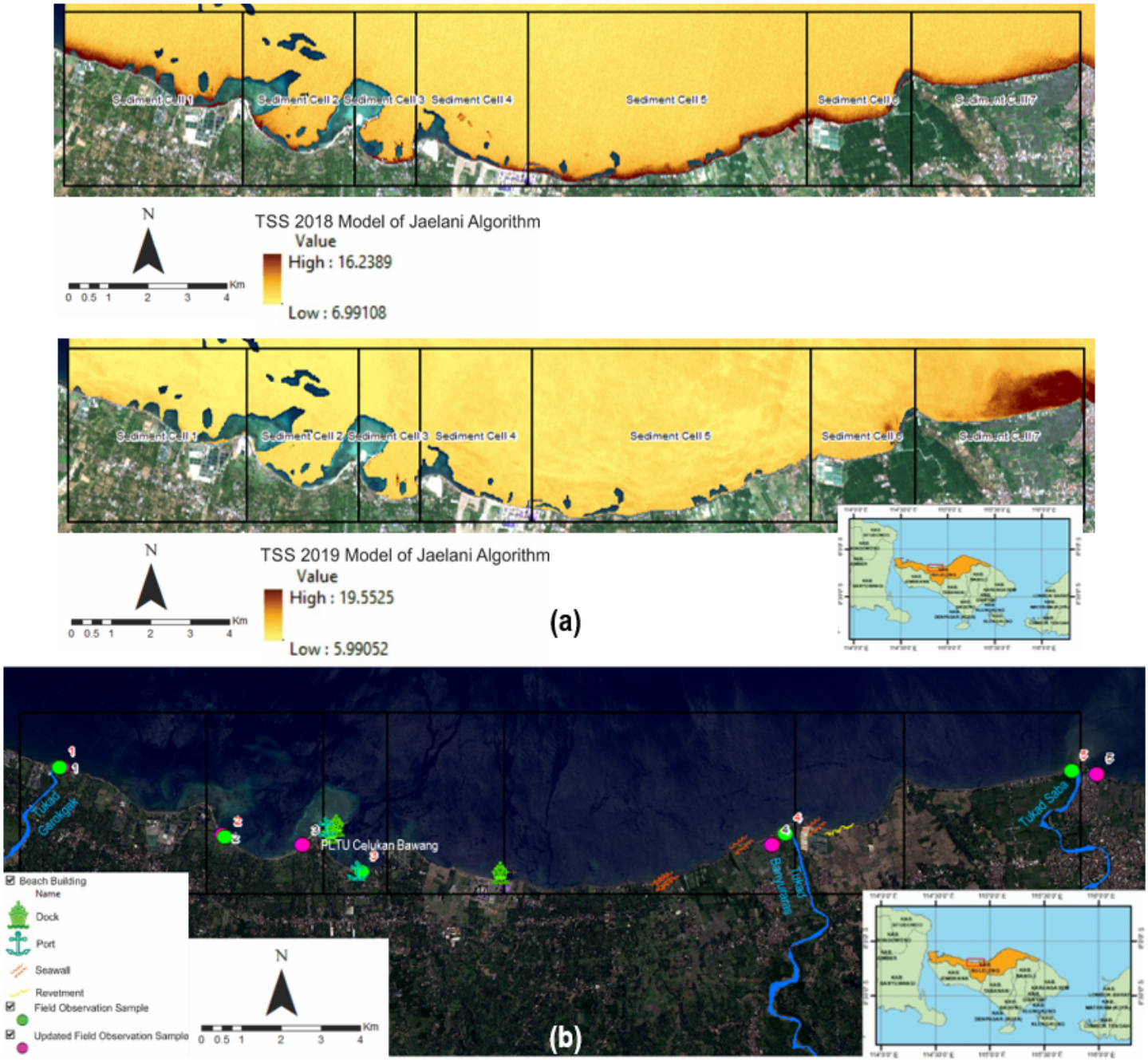

Figure 4

(a) TSS modeling using the Jaelani Algorithm on level-2A Sentinel images in 2018 and 2019; and (b) Building distribution along the beach, with a SPOT-7 image on the background (Source: Center for Coastal Research and Development, Ministry of Public Works and Housing, 2019)

Figure 5

Piles of garbage in the Tukad Gerokgak (a) and Tukad Saba (b) estuaries. Tukad Gerokgak estuary at 08:00 in the morning (c) and 05:00 in the afternoon (d)

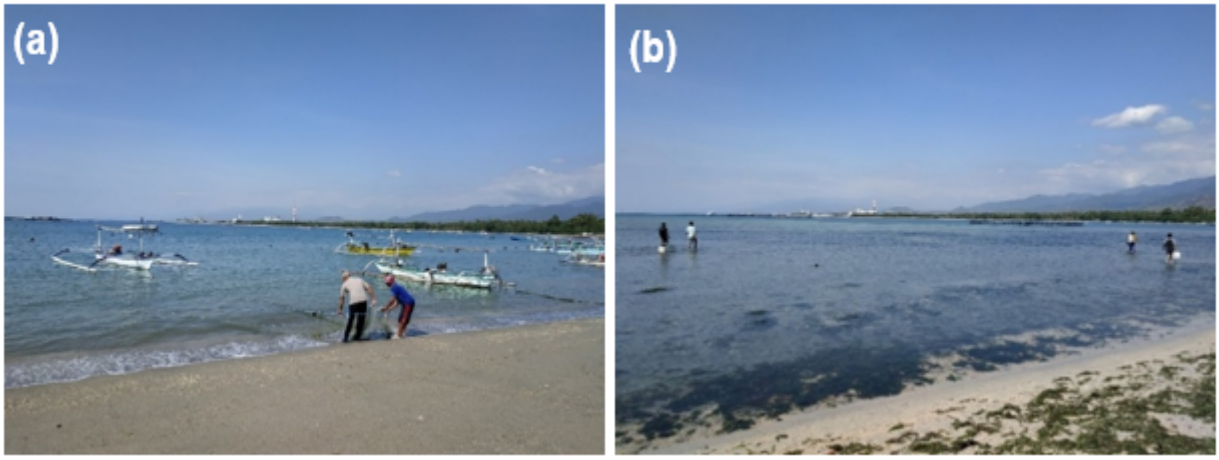

Figure 6

Tide variation on Nusantara Beach at 09:00 in the morning (a) and 04:00 in the afternoon (b)

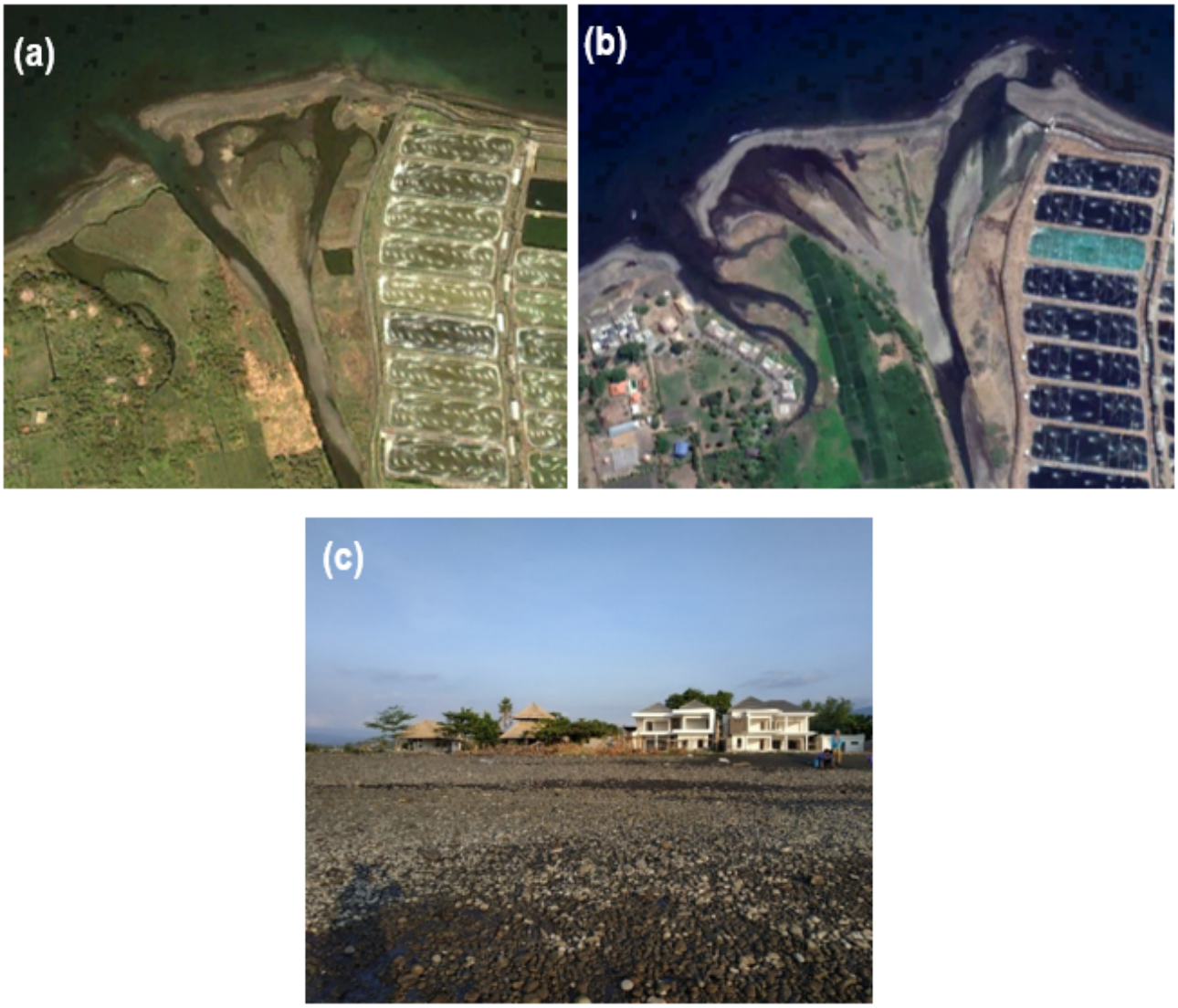

Figure 7

Dynamics of the Tukad Banyuraras estuary on December 12, 2013 (a), and August 20, 2019 (b), and resort construction in 2019 (c)

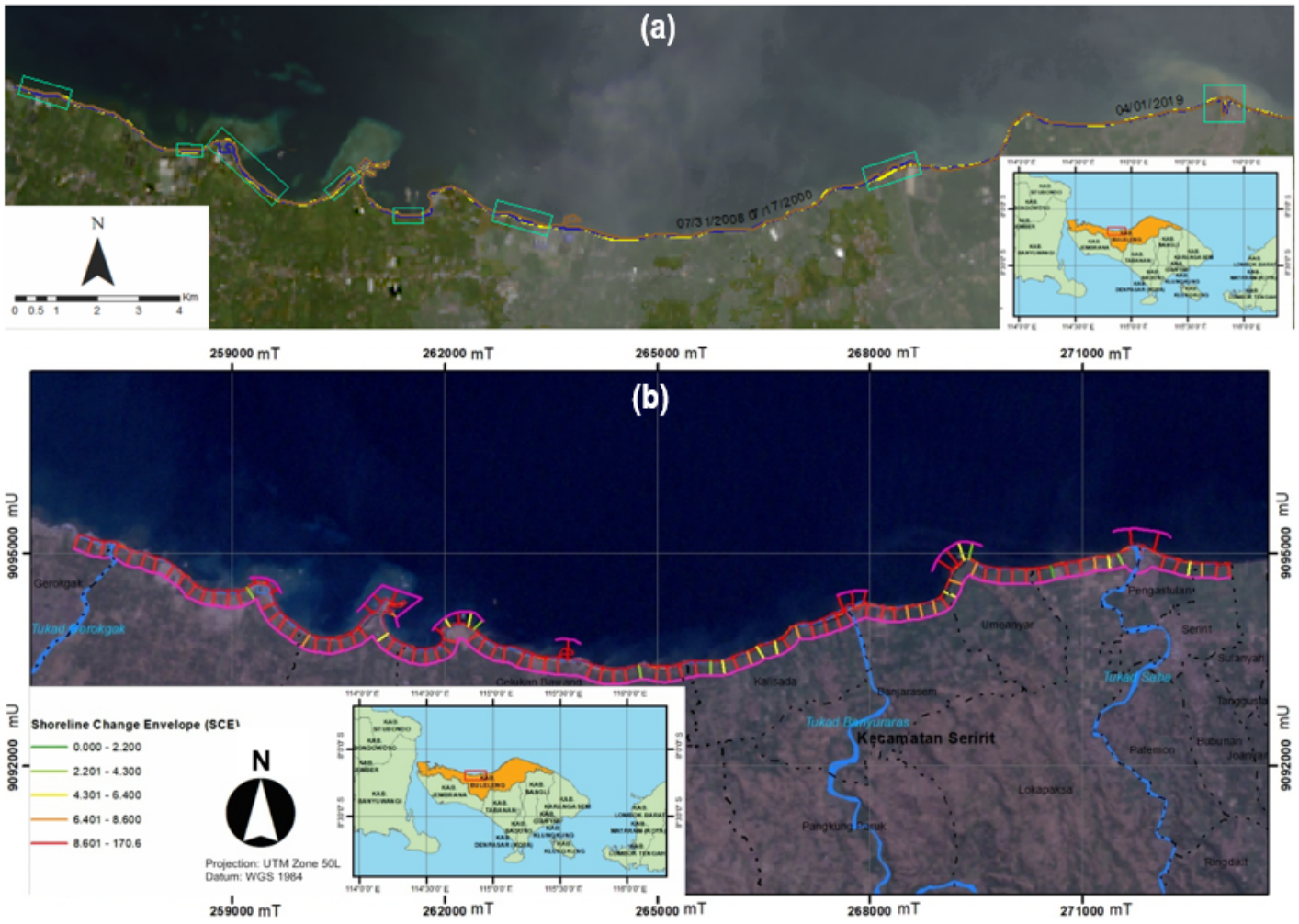

Figure 8

(a) Significant shoreline shifts in 20 years (2000–2019) identified from Landsat images; and (b) Map of shoreline changes identified from Landsat images (Source: Wicaksono & Winastuti, 2020)

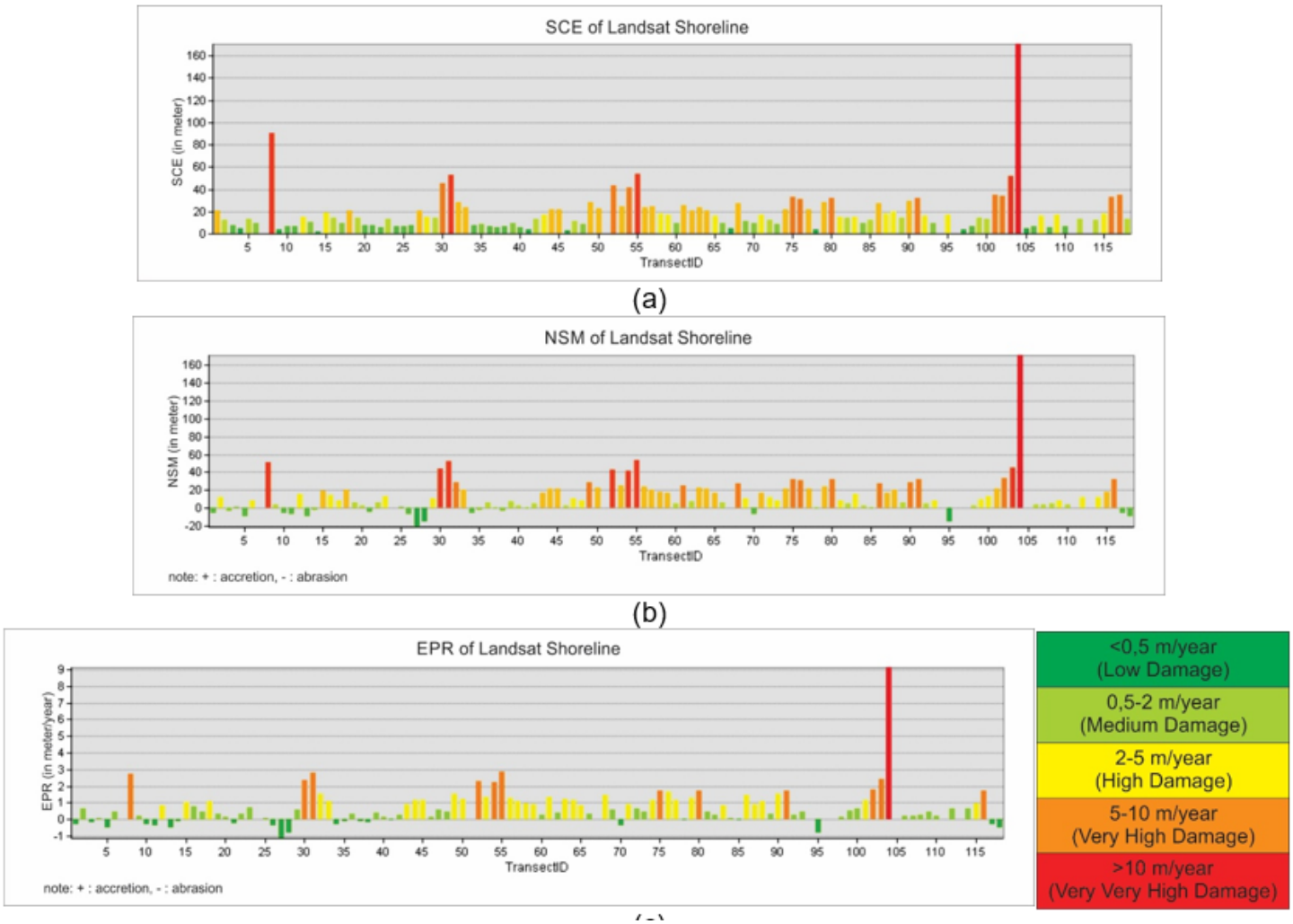

Figure 9

Graphs of shoreline changes in 20 years (2000–2019), as identified from Landsat images using statistical tools: (a) SCE, (b) NSM, and (c) EPR (Source: Wicaksono & Winastuti, 2020).

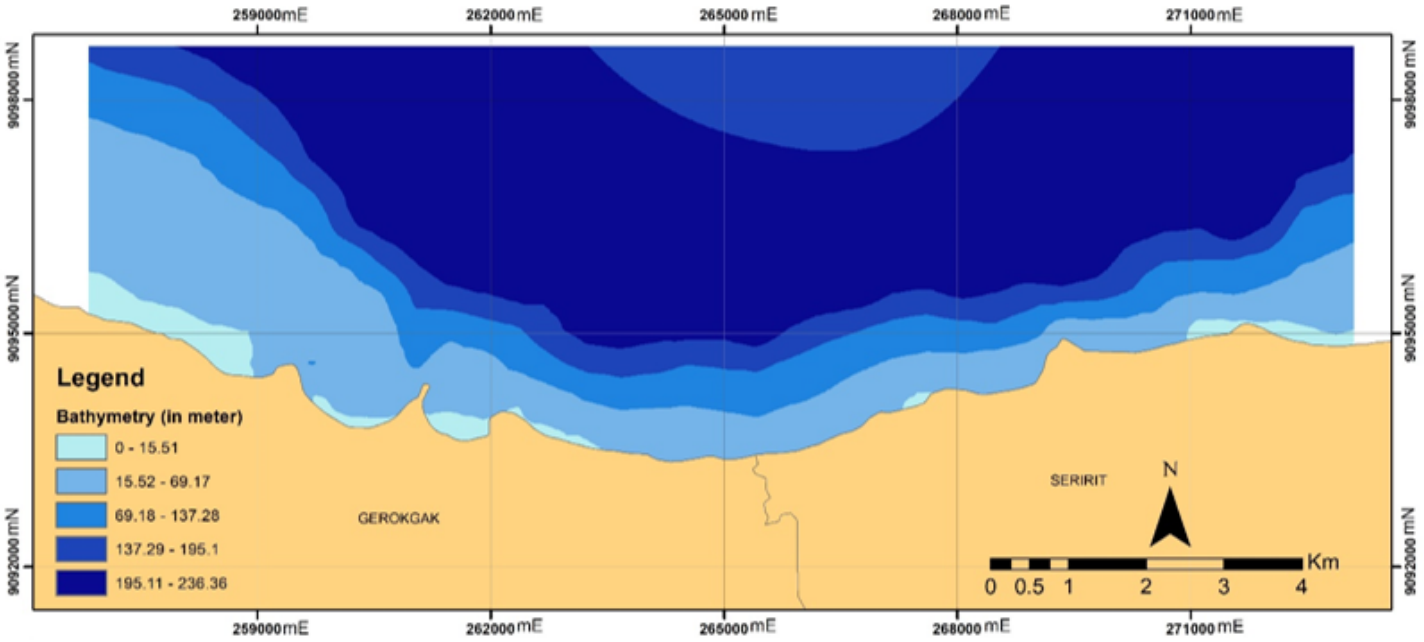

Figure 10

Bathymetry map of the Buleleng waters

Figure 11

Residential buildings and coastal defense structures